Valence Photoionization of Thymine:
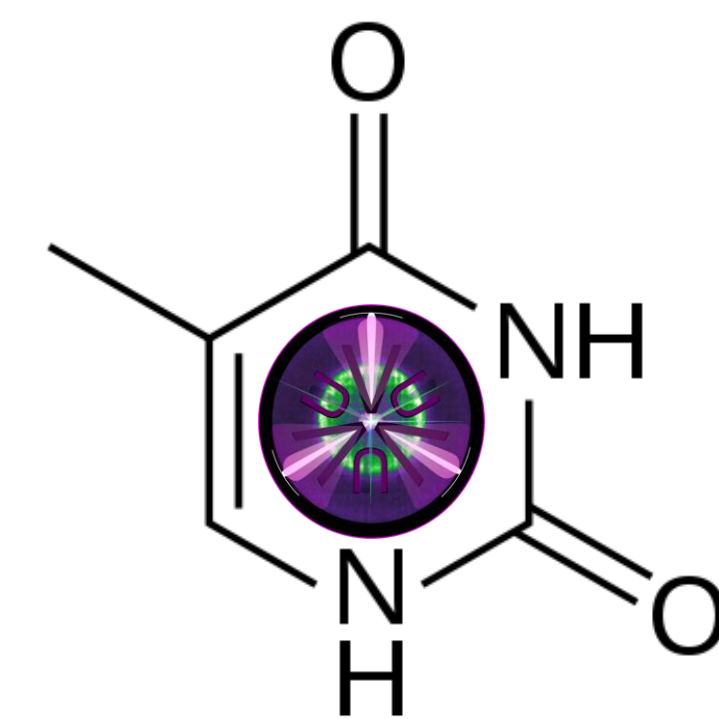# Ionization Energies, Vibrational Structure,
& Fragmentation Pathways from the Slow to the Ultrafast

PAUL SCHERRER INSTITUT

ETH zürich

Katharina Majer,[a,b] Ruth Signorell,[a] Maarten Heringa,[b,c]
Maximilian Goldmann, Patrick Hemberger,[b] and Andras Bodi[b],*

[a] Department of Chemistry and Applied Biosciences, Laboratory of Physical Chemistry, ETH Zürich 8093 Zürich, Switzerland; [b] Paul Scherrer Institute, 5232 Villigen, Switzerland

1 Motivation

The photophysical and –chemical properties of DNA bases form the basis to understand their reactivity. This is of special interest in a diverse range of research areas from the examination of mutagenic and carcinogenic effects of photoinduced structural changes to DNA to sample damage in crystallographic structure determination of macromolecules or in the pursuit of understanding the molecular origins of life. The presence of purines and pyrimidines in Comet Halley suggests that these molecules were transported to Earth by cometary dust. The study of VUV radiation effects on DNA bases may thus shed light on their possible genesis and survival under extreme conditions.

2 PEPICO endstation at VUV beamline (SLS) [1]

- Internal energy selection by photoionization and by tuning $h\nu$
- Velocity map imaging to select zero kinetic energy electrons
- Mass analysis → fractional parent and daughter ion abundances as a function of $h\nu$ → BD
- Decay rate measurements $10^3 < k/s^{-1} < 10^7$

3 Results and discussion

Ionization Energies & Vibrational Structure:
Threshold Photoelectron Spectrum (TPES)

bulk evaporation
aerosol vaporization
FC simulation
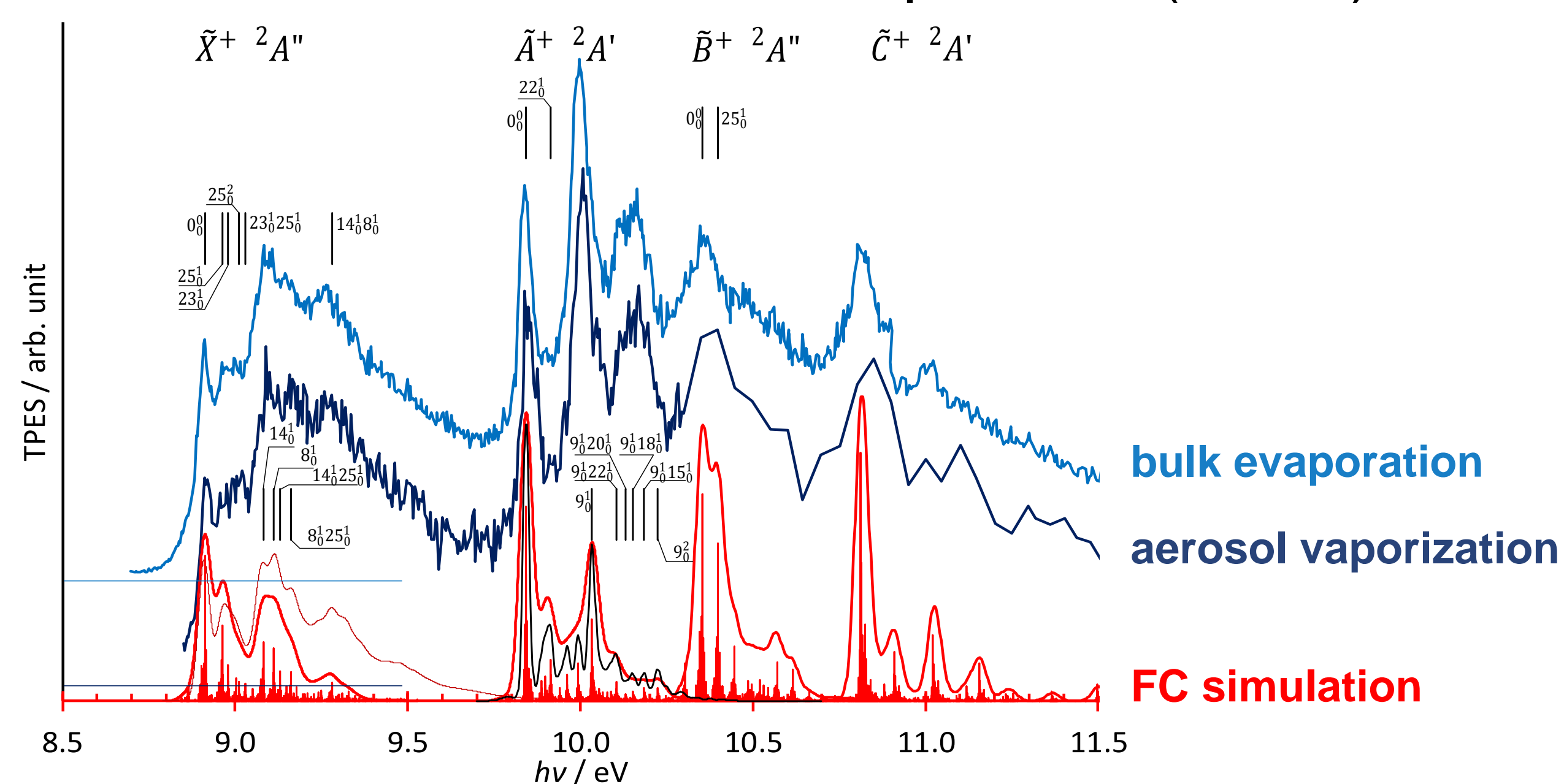
Franck–Condon factors (FCFs) for vibrational transitions are convoluted with a Gaussian to account for thermal broadening.
Apart from the better S/N ratio for bulk evaporation, the evaporation technique does not have significant impact on the TPES fine structure, implying similar rotational temperature in both cases. **Comparing our assignments of vibrational transitions with the literature [2,3] highlights the value of FC simulations**: We agree with previous assignments relying on FC simulations (X^+) [3] and disagree with the others (A^+) [4].

IE [eV]	experimental		theoretical	
	this work	literature	this work [a]	literature
$X^+\ {}^2A''$	8.922 ± 0.008	8.9178 ± 0.0010 [2] 8.913 ± 0.005 [3]	8.842	8.917 [3],b
$A^+\ {}^2A'$	9.851 ± 0.008	9.842 ± 0.005 [4]	9.892	9.868 [4],b
$B^+\ {}^2A''$	10.30 ± 0.02		10.285	
$C^+\ {}^2A'$	10.82 ± 0.01		10.869	

[a] (EOM-IP-)-CCSD/cc-pVTZ with (EOM-IP-)-CCSD/cc-pVDZ ZPVE, [b] (R)CCSD(T)F12(b)/cc-pVTZ-F12 (+CV+SR+ZVPE)

### Fragmentation Pathways: Breakdown Diagram (BD)
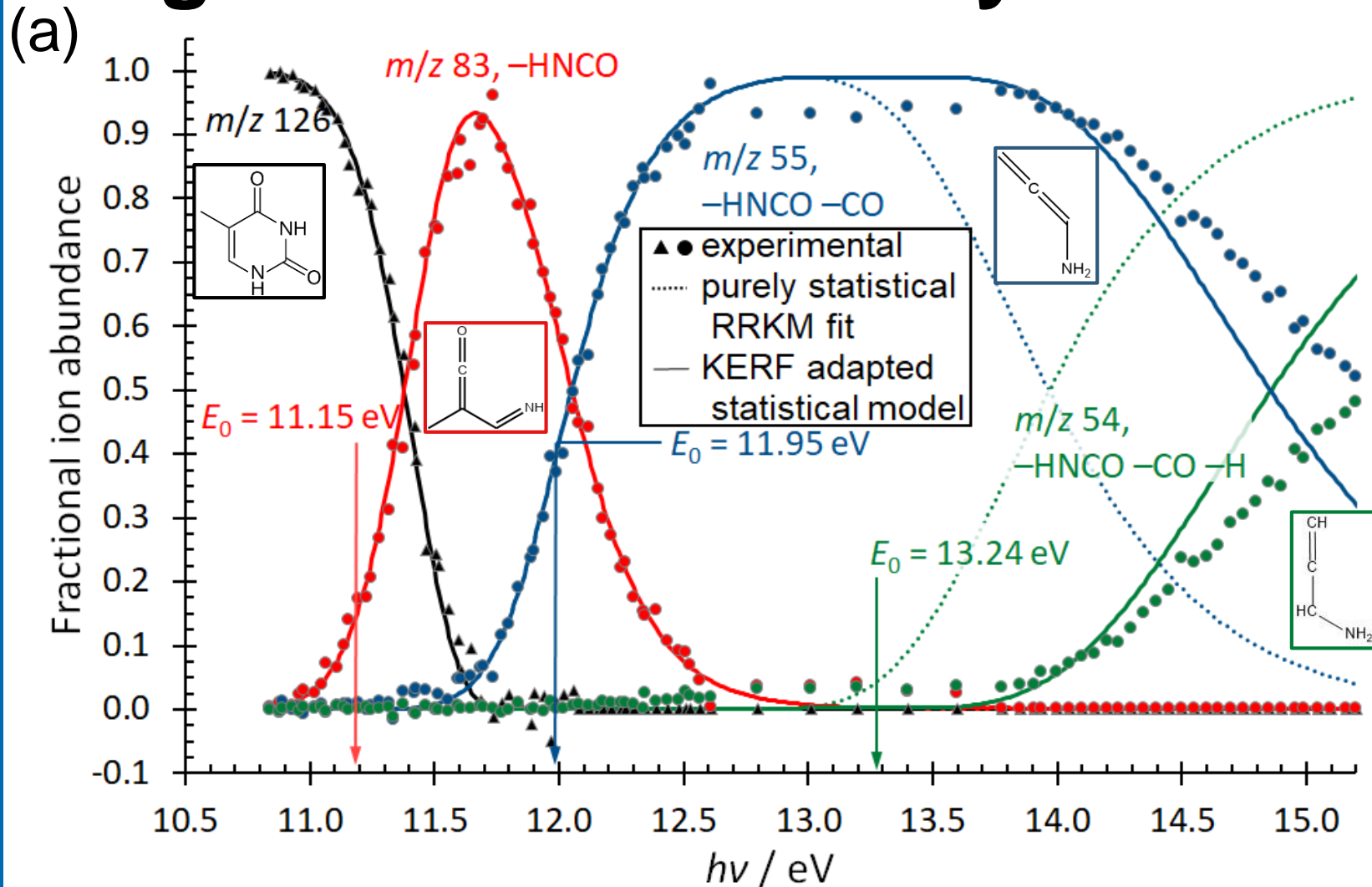
a) We assumed the Boltzmann distribution's transposition of the neutral's internal energy into the ion manifold in the statistical fit. Fitting parameters: temperature T, dissociative photoionization threshold E_0. Above E_0 the parent ion fragments. For the last dissociation step yielding m/z 54 the purely statistical model does not hold, because the previous dissociation leading to m/z 55 is impulsive (see PES). → More internal energy is released as kinetic energy of the fragments than assumed by the purely statistical model.
→ Adaption of the model: Assume constant kinetic energy release factor (KERF): remove one translational degree of freedom from the statistcal calculation of the product energy, rescale BD in the photon energy range of H loss ($h\nu > 12.99$ eV) as follows:

$$E(\,h\nu > 12.99\ \text{eV}) = 11.15\ \text{eV} + \frac{h\nu - 11.15\ \text{eV}}{1 - \text{KERF}}, \qquad \text{KERF}_{opt} = 0.24$$
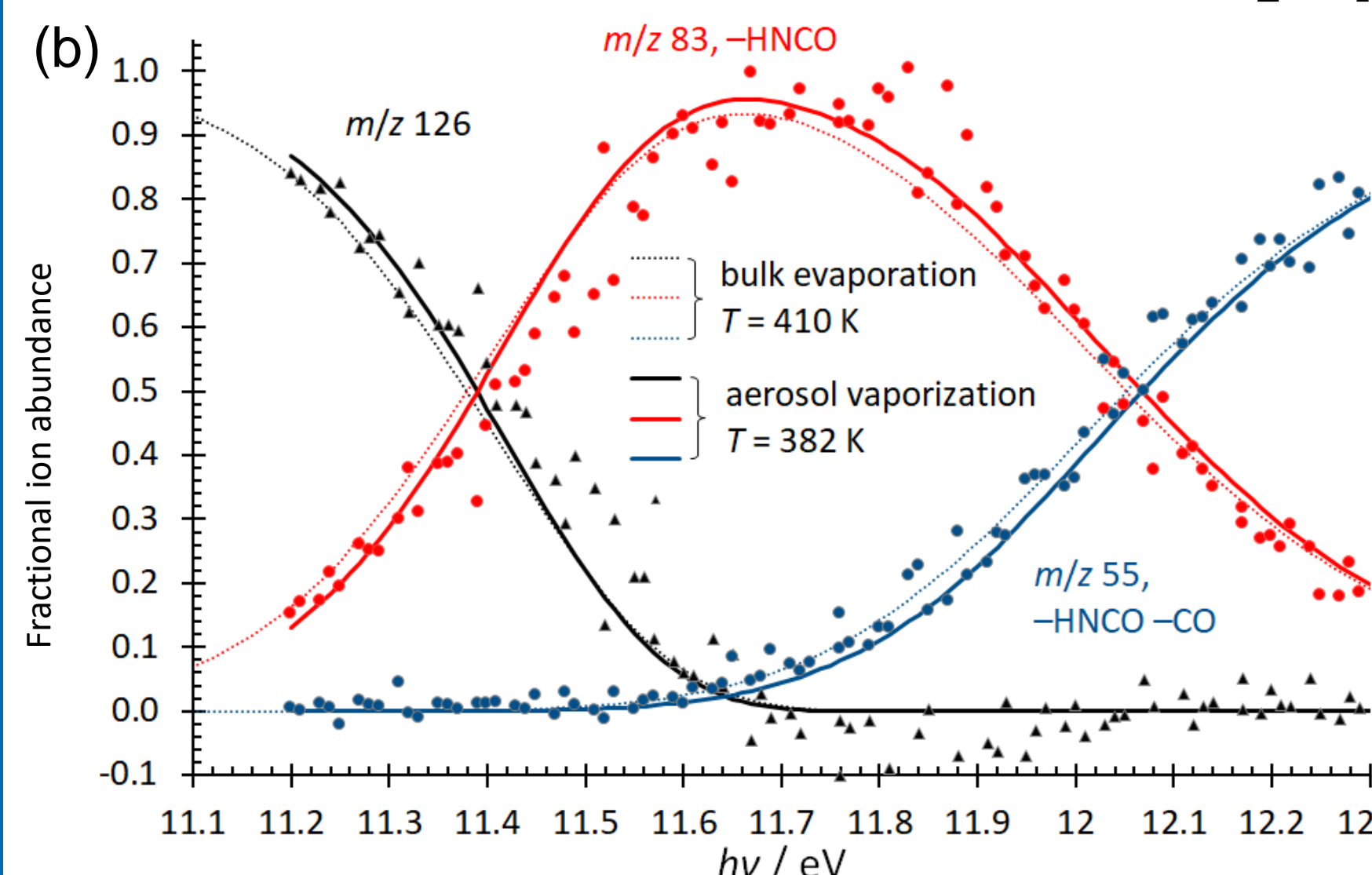
b) The difference in the final internal energy achieved by bulk evaporation or aerosol vaporization was quantized based on the statistical model: For bulk evaporation the best fit model was found to correspond to a temperature of 410 K. This model was then fitted to the BD based on data from aeorosol vaporization by varying only the temperature T. For both methods the same thermodesorber temperature of 390 K was used.
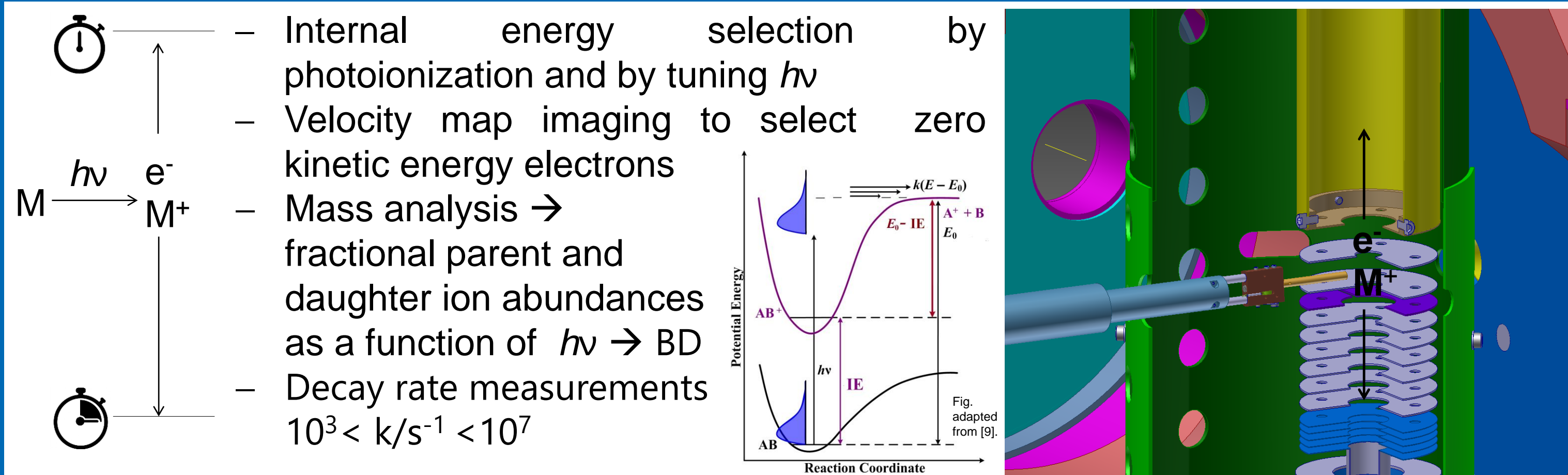
Low temperature difference in the two methods → the mildness of aerosol vaporization results in part from the suppression of condensed-phase pyrolysis processes.

Fragmentation Pathways: Potential Energy Surface (PES)

Reaction energy profile for thymine cation fragmentation. **Black**: likely active dissociation pathways. Grey: previously proposed, [5-7] but energetically or kinetically unlikely pathways. Dotted: submerged intermediate transition states and minima, e.g. the first dissociation takes place over such a barrier, 100 meV below the threshold. Dashed: only reaction energy is shown.

The **exploration of the PES is guided by mechanistic insights from the BD** and the assumption that internal conversion is fast compared with fragmentation, and thus dissociation takes place on the ground state PES. This assumption is supported by increasing peak width and dissapearing fine structure in the excited state TPES bands hinting at short excited state lifetimes. The first fragment, m/z 83, is formed via retro-Diels-Alder mechanism followed by H transfer. Potentially it could isomerize to one of numerous more stable products, but as the barrier for sequential CO loss is comparably low, this is unlikely. Above ca. 13.8 eV sequential H loss insignificantly competes with CO loss. This may be due to a looser H-loss transition state compared with the isomerization transition state of CO loss or due to H-loss from a more stable m/z 83 isomer. For CO loss our calculations suggested internal rotation around the C-CH bond followed by a five membered ring transition state (see starred structure) as the most plausible mechanism. Simple C=C bond breaking was found to involve a transition state incompatible with the CO loss onset. The blue rectangle in the figure above shows isomers of m/z 55 which may interconvert depending on the available internal energy.

From Slow to Ultrafast
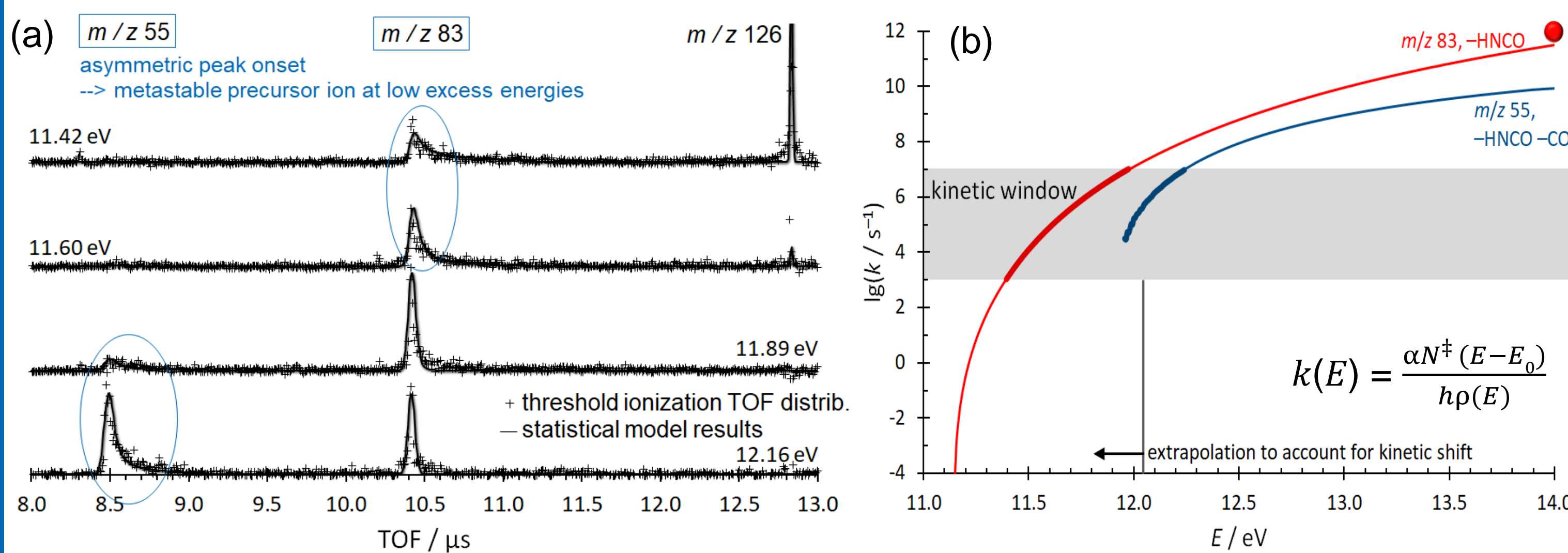
b) Modeled rate curves for HNCO and CO loss as function of the internal energy of the respective parent ion. The internal energy is given relative to the neutral ground state. The red dot denotes the HNCO-loss rate determined by time-dependent Auger spectroscopy at the maximum attainable energy after three photon absorption. [8] This agrees well with the extrapolation of the rates we measured within the kinetic window. **The time scales in question are commensurate with energy dissipation times expected for the condensed phase**, be it ices or biological systems, which implies that the fragmentation processes observed here may be fast enough to occur in these contexts, too.

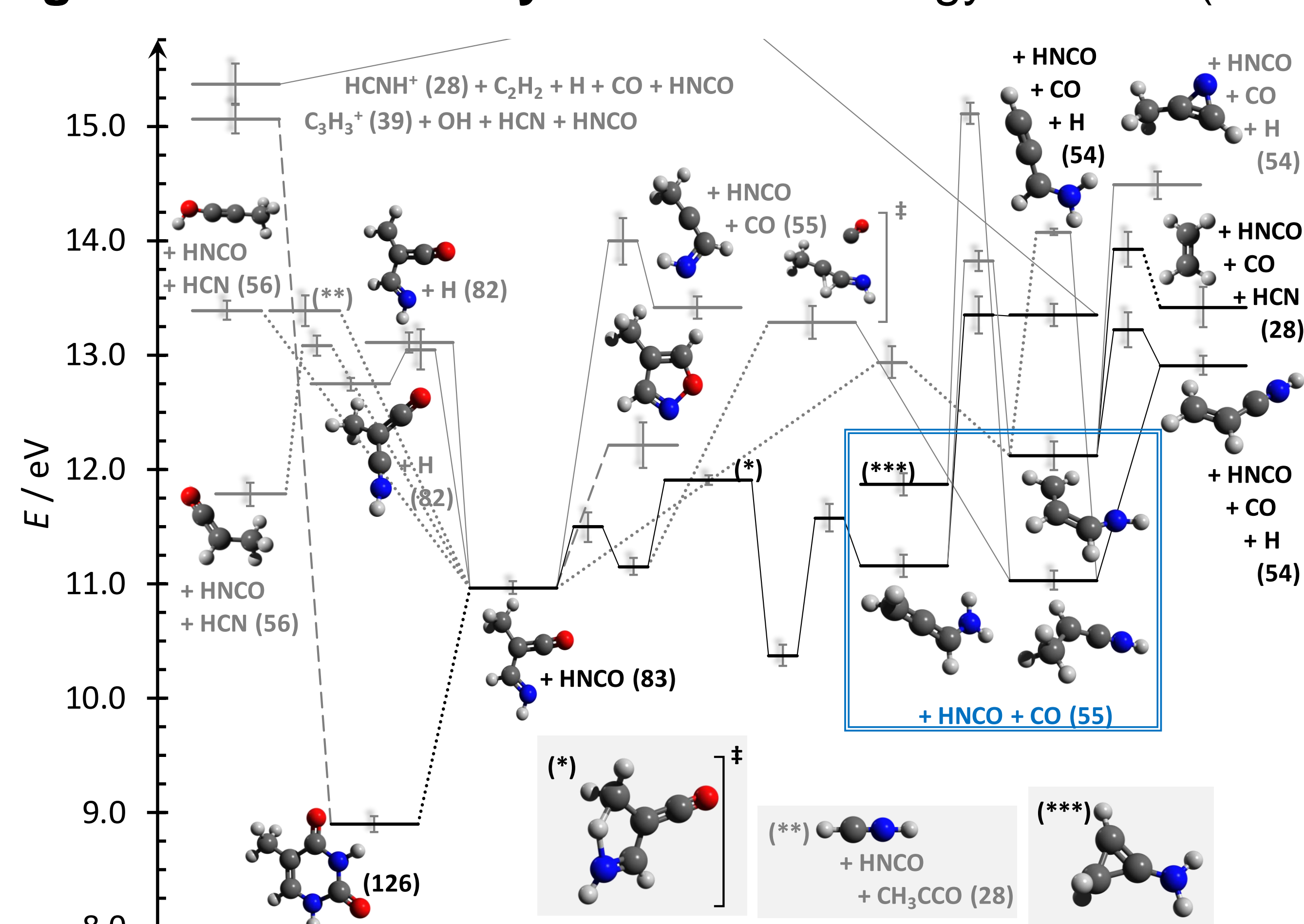$$k(E) = \frac{\alpha N^{\ddagger}(E - E_0)}{h\rho(E)}$$

4 Further conclusions

Regarding astrochemical aspects, we confirm that thymine does not dissociatively ionize at the Lyman-α line (10.2 eV), but it may form neutral fragments. → Its survival depends on radiation shielding environments.
Inverse processes may indicate potential ion chemistry synthesis pathways.

5 References

[1] M. F. Heringa et al., *ChemPhysChem* **2017**, 24, 3595.
[2] K.-W. Choi et al., *J. Am. Chem. Soc.* **2005**, 127, 15674–5.
[3] Y. Majdi, M. Hochlaf et al., *J. Phys. Chem. A* **2015**, 119, 5951–8.
[4] M. Hochlaf, Y. Pan et al., *J. Phys. Chem. A* **2015**, 119, 1146–53.
[5] H. W. Jochims et al., *Chem. Phys.* **2005**, 314, 263–82.
[6] J. M. Rice et al., *J. Am. Chem. Soc.* **1965**, 87, 4569–76.
[7] C. A. Bauer, S. Grimme, *Eur. J. Mass Spectrom.* **2015**, 21, 125–40.
[8] T. Wolf, F. Holzmeier et al., *Appl. Sci.* **2017**, 7, 681.
[9] J. Harvey, from Wikimedia Commons (https://creativecommons.org/licenses/by-sa/3.0, 04.06.2018).